A Free Viewpoint Portrait Generator with Dynamic Styling

Anpei Chen*   Ruiyang Liu*   Ling Xie   Jingyi Yu

{chenap,liury,xieling,yujingyi}@shanghaitech.edu.cn

Abstract

Generating portrait images from a single latent space facing the problem of entangled attributes, making it difficult to explicitly adjust the generation on specific attributes, e.g., contour and viewpoint control or dynamic styling. Therefore, we propose to decompose the generation space into two subspaces: geometric and texture space. We first encode portrait scans with a semantic occupancy field (SOF), which represents semantic-embedded geometry structure and output free viewpoint semantic segmentation maps. Then we design a semantic instance wised(SIW) StyleGAN to regionally styling the segmentation map. We capture 664 3D portrait scans for our SOF training and use real capture photos(FFHQ[12] and CelebA-HQ[16]) for SIW StyleGAN training. Adequate experiments show that our representations enable appearance consistent shape, pose, regional styles controlling, achieve state-of-the-art results, and generalize well in various application scenarios.

1. Introduction

Quality, variety and controllability are three main concerns in portrait image generation. People may expect the generator to maximize the quality and variety of generated images while allowing a certain degree of semantically meaningful user control, such as free-view synthesis or style adjustment for a specific region. While we've seen rapid improvement in quality and variety of images produced by Generative Adversarial Networks(GANs)[6, 12, 13], controlling the generation according to user preference is still under exploration, especially preserving the overall style-consistency while adjusting a specific attribute.

The state-of-the-art GAN-based unconditional image generator StyleGAN2[13] scales image features at each Conv layer based on the incoming style, and achieve promising controlling over intuitive coarse (contour), medium (expressions, hairstyle) and fine levels (color distribution, freckles). However, as such control is scale-specific, semantically well-defined attributes are still coupled in different scales, making it impossible for attribute-specific control. For example, expression and hairstyle would change along with head pose, as they are entangled in the same medium scale.

Seminal researches[2, 29] explore to decompose the generation space of StyleGANs into attribute specific bases, i.e., direction codes, and control the generation by dragging the random style code toward each attribute direction. Such decomposition assumes attributes are orthogonal to each other in the original generation space, which is indefensible, thus generally leads to flicking and undesirable attributes change during generation.

A recent line of works seek 3D priors for help [33, 5], and achieve convincing facial animation and relighting results with explicit user control. However, constraint by the representing ability of explicit 3D facial priors (most commonly, the morphable model), they may fail to model decorative attributes, like hair, cloth, etc. Most recently, Zhu et. al. [38] proposed a *Semantic Region-Adaptive Normalization (SEAN)* layer to enable regionally style adjustment conditioned on a segmentation map. Thought to push the frontier even further in both image synthesis and editing, the requiring of pair-wise training data limits the power of their method in actual applications where pairing data is hard to acquire.

Instead of disentangling from the pre-trained generation space, we model the generation procedure with two individual latent spaces to enables more specific attribute-wise control over the generation. Inspired by recent works on implicit geometric modeling[18, 31, 20, 3], we extend the signed distance field as a *semantic occupancy field(SOF)* to model portrait geometric. *SOF* describes the probabilistic distribution over k semantic classes (including hair, face, neck, cloth, etc.) for each spatial point. To synthesis images from SOF, we first project *SOF* onto 2D segmentation maps with user-specified viewpoints, then we paint each semantic region with a style code sampled from the texturing space. We propose a *semantic instance wise (SIW)* StyleGAN for texturing to support dynamic regional style control. Specifically, we design a novel semantic-wised "demodulation" and a spatially mix style training scheme to mix two random style codes for each semantic region during training. We further encode semantic segmentation map to a low dimensional space with a three-layer encoder to encourage

continuity during view changing.

We evaluate our method on FFHQ[12] and CelebAMask-HQ dataset[16], our generator achieves a lower Frchet Inception Distance (FID score) than the SOTA image synthesis methods. We will release our code, pre-trained models and results [1].

To summarize, we proposed a photo-realistic portrait image generator, which supports

- **Free viewpoint generation.** Our framework grants direct control of portrait geometry and is able to generate view consistent images under arbitrary viewpoint.

- **Semantic-level adjusting.** Our generator enables us stylizing each semantic region separately, thus able to globally and locally generate, adjust, or transfer styles of the generate image.

- **None-pairwise training.** Our SIW StyleGAN relax the pairwise constrain between semantic maps and images, allows us to train network with synthesis semantic data and real capture images, thus enable us to separately train the *SOF* and *SIW StyleGAN*,

2. Related Work

Unconditional image generation. The computer vision and graphics community have made significant progress in high-quality conditional image synthesis, especially after the seminal work of generative adversarial networks[6] (GAN) by Goodfellow et al.[12, 13, 9, 35, 20, 32]. To synthesis high-resolution images, ProgressiveGan[11] introduces a training method that grows both generator and discriminator progressively, which not only can generate high-resolution results but also speed up and stabilize the training progress. While following work StyleGANs[12, 13] redesign the generator architecture in a exposes novel ways to control the image synthesis process. The generator starts from a constant learned input and adjusts the style at each convolution layer, therefore directly controlling the strength of image features at different scales, e.g., unsupervised separation of high-level attributes (e.g., pose, identity) from stochastic variation (e.g., freckles, hair), and enables intuitive scale-specific mixing and interpolation operations. It not only brings state of the art results but also demonstrates a more linear, less entangled representation of variation.

The scale-specific effects of the StyleGAN2 are too rough and the same scale's attributes are generally mixed together. Instead of dividing image synthesis into coarse/median/fine scale style controlling, we regards the generation as drawing on different semantic region, thus we re-modeling images synthesis as regionally stylize procession, which enables us to explicitly control output's contour and individually adjust both global and local image styles.

Conditional image generation. In most cases, conditional image synthesis aims at learning a mapping from condition to target images, condition mostly are labels or images[10, 36, 21, 38]. Pix2Pix [10] first model image-to-image generation with an U-Net[25] architecture, they first encode condition images into a high level feature space and then decoding, regress with both VGG [30] perceptual feature loss and GAN loss. To address that adversarial training might be unstable and prone to failure for high-resolution image generation tasks, Pix2PixHD[36] design a multi-scale generator and discriminator architectures to produce higher resolution images. However, the condition image would generally vanish/explode gradients as the network gets deeper, thus SPADE[21] propose using a spatially-adaptive normalization process to each decoding layer instead of only to the beginning of the network. Most recently, SEAN[38] attempts to synthesis style specified images by combining style latent vector and semantic maps, which reaches SOTA FID score. However, they are both heavily rely on perceptual loss[30], which result in, on the one hand, require pairwise condition vs. target images, on the other hand, generating high-resolution images usual lacking fine details, realistic textures and rich texture styles.

Latent space manipulate. However, common unconditioned GAN architecture generally maps latent code and synthesis images from random gaussian noise. They can not explicitly control and synthesize semantic specific attributes(e.g., pose, eye, age for human portrait). Since the disentangled representation is discovered[34, 27, 15] in common VAE, GANs[11, 12] architecture, many studies on latent space[33, 28, 24] that observes the vector arithmetic phenomenon have been engaged in changing the attributes of output images. Shao et. al. use linear SVM [28, 4] to classify the latent code with a corresponding semantic label. Most recently, Tewari et. al.[33] combine 3DMM[1] priors and rendering procedure into adversarial learning, and the controlling synthesis produces with low dimensional parameters. These pretrained-gan-based methods' performance highly depends on the coupling and linearity of attribute distribution in the latent space. For example, the elder(age attribute) are more tended to wear glasses(glass attribute). In addition, under the setting of stylegan, unrelated semantic attributes are also likely to couple due to generator architecture that use style vectors in different layers to control the information under different frequency. For example, changing the pose will also cause hairstyle, face to shift and prone to artifacts.

Implicit geometric modeling. Our representation is more related to most recent implicit fields modeling[20, 20, 3, 18], which attempt to represent an object's surface with a signed continuous distance function/field, where the signed(-/+) indicates a region whether inside the object. Similar to 2D classifier[30], the signed fields are well suit-
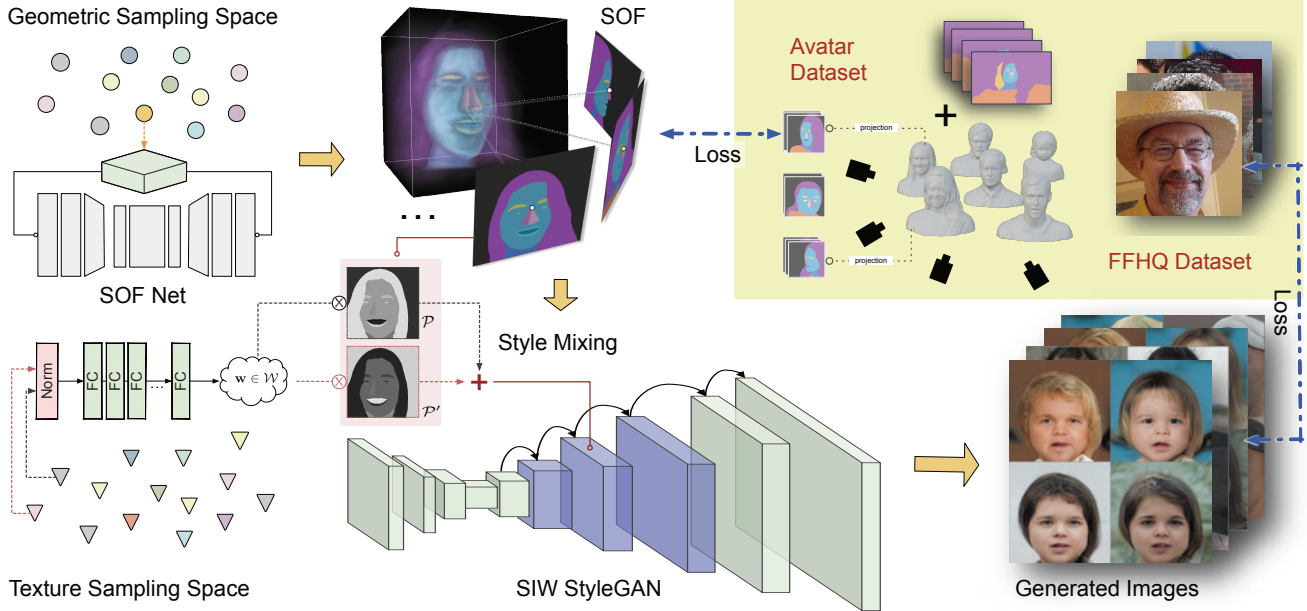
Figure 1. Pipeline. From left to right: The two sampling spaces; The *semantic occupancy field (SOF)* used for geometric modeling and the *semantic instance wise generator (SIW)* used for texturing; Datasets used for training and generated results, the Avatar dataset is built from a set of 3D facial models and segmentation texture maps. We project each model to 20 views to creates 2D segmentation maps for training.

able for network regression due to its continuity. Unlike most 3D geometry modeling require 3D supervision, our semantic occupancy field implicitly learns 3D semantic label boundary from a set calibrated segmentation maps, the training maps can be either comes from synthesis rendering or real capture multi-view images.

3. Overview

We decouple the generation space into geometric space $\mathcal{G}_{SOF}$ and texture spaces $\mathcal{G}_{SIW}$. Inspired by the graphics pipeline, we first generate 3D geometry from the geometric space then project it onto 2D for texturing. Projecting 3D geometry onto 2D space may cause 2D discontinuity (i.e., holes), leading the gradient to vanish if we want to train the generator in an end-to-end way. Thus, we represent the geometric structure of a portrait scan as a contiguous 3D semantic probability field, i.e., *semantics occupancy field (SOF)* to enable both free-view generation and regional styling. We modify the scene representation network [31] to encode each *SOF* into a vector $z \in \mathbb{R}^{256}$ in the geometric space $\mathcal{G}_{SOF}$. We project *SOF* into 2D segmentation maps with explicitly specified camera poses for texturing.

The texturing stage is based on a semantic instance wised (*SIW*) StyleGAN. *SIW* is a painter who paints portrait texture onto a given segmentation map refers to a style code sampled from the texturing space. Since the contour of each style region is explicitly specified by the segmentation map, we can achieve both global and local texture adjust-

ment with a single *SIW* generator. The whole generation procedure is formulated as:

$$
\begin{aligned}
\mathcal{I} &= G(z_t, Proj(\mathcal{S}_{z_g}, C)))) \\
z_t, z_g &\in \mathcal{G}_{SIW}, \mathcal{G}_{SOF}
\end{aligned}
\tag{1}
$$

Where the z_g, z_t are latent vectors sampled from the SOF geometric space and SIW texturing space respectively, $C = [R, T | K]$ represents a user-specified viewpoint.

In the following, we first introduce *SOF* formulation, generation of the geometry space $\mathcal{G}_{SOF}$ and how to sample free-view semantic segmentation maps of geometric-varying instances from $\mathcal{G}_{SOF}$. Then in sec.5, we describe the architecture of SIW-StyleGAN to support regional texturing from segmentation maps.

4. Geometric modeling with SOF

Implicit 3D representation defines a surface as a level set of a function $\mathcal{F}$, most commonly the set of points that satisfy $\mathcal{F}(x) = 0$, where the value of $\mathcal{F}(x)$ is often referred to as the signed distance function (SDF). A recent stream of works explores to approximate $\mathcal{F}$ with neural networks and achieves the state-of-the-art performance on both 3D reconstruction and free-view rendering [19, 26, 23, 20].

However, surface properties cannot be well-represented by a single SOF as it only describes geometric without any semantic information. We extend the range of the function to a more general k-dimensional vector that describes cer-
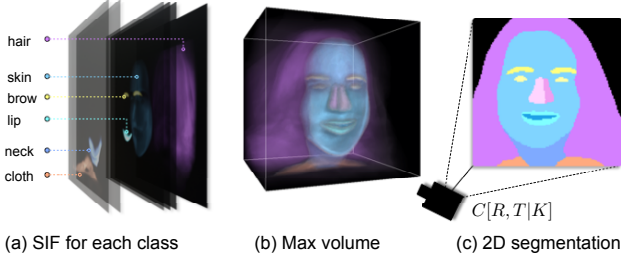
Figure 2. Visualization of *SOF*. Here *SOF* is treated as a $(H \times W \times D \times K)$ volume, with $\mathcal{S}(p)$ as density, and visualized by volume rendering. (a) Rendered semantic probability field for each class s_i with p_{s_i} as volume density. (b) Softmax volume after applying $argmax(\cdot)$ to P_s, we use color to represent segmentation result, and max probability as density. (c) We generate 2D semantic segmentation map by querying the max volume with rays shoot from a given camera.

tain properties for each spatial location with a neural approximation:

$$\mathcal{S} : \mathbb{R}^3 \to \mathbb{R}^k, \quad p(x,y,z) \mapsto \mathcal{S}(p(x,y,z)) \qquad (2)$$

4.1. Semantic Occupancy Fields

In the free-view image generation scenario, a suitable property vector should preserve the geometric consistency under arbitrary viewpoints; secondly, preserve high-level neighborhood structure, so that the style within each neighborhood is consistent and could be represented by a single style code for texturing.

Thus in *SOF*, we define the property vector as occupancy probability distributed among k semantic classes, and assign for each spatial location $p(x,y,z)$ a k-D vector P_s in $[0,1]$ with

$$\mathcal{S}(p(x,y,z)) = P_s = \{p_{s_i} | i = 0, 1, ..., k-1\}$$

$$\text{with } p_{s_i} \in [0,1] \text{ and } \sum_{i=1}^{k} p_{s_i} = 1$$

where p_{s_i} refers to the probability of semantic region s_i occupying spatial point $p(x,y,z)$.

To obtain 2D segmentation maps for the texturing stage, we querying $\mathcal{S}$ with rays shoot from a given camera $C[R,T|K]$ and a estimated per-pixel depth value d. Fig. 2 gives a visualization of *SOF* together with corresponding views' 2D segmentation map.

4.2. Architecture

Inspired by most recent works on neural scene representation [31, 20, 3], we implicitly represent SOF with two Multi-layer perceptrons (MLPs): Φ and Θ. Φ is used to
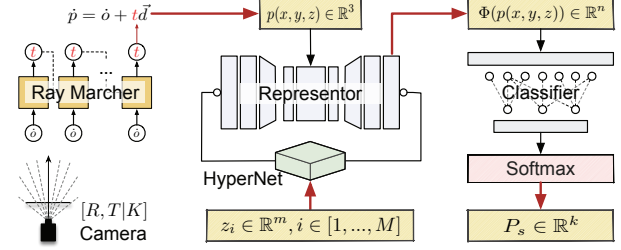

Figure 3. *SOF* contains three modules. A ray marcher (left) predicts depth for each camera, to identify a sample point $p(x,y,z)$ for each ray. For each instance we use a scene representer Φ (middle) to map p into a feature vector $f_p \in \mathbb{R}^n$ that describe the spatial properties on p. Φ is generated from latent code z_i via a hyper network [7]. Finally, the classifier (right) predicts a k-class distribution as the final *SOF* output P_s.

encode semantic properties of each spatial location p into a feature vector $f \in \mathbb{R}^n$, while Θ is a semantic classifier following a softmax activator to decode feature f into the above k dimentional probability P_s, i.e

$$\Phi : \mathbb{R}^3 \to \mathbb{R}^n, \quad p(x,y,z) \mapsto \Phi(p(x,y,z))$$
$$\Theta : \mathbb{R}^n \to \mathbb{R}^k, \quad \Phi(p(x,y,z)) \mapsto P_s \qquad (3)$$

To train *SOF*, we first capture 664 portrait scans and render a set of 2D semantic segmentation maps for each instance with random camera poses. We jointly optimize Φ and Θ by projecting *SOF* to each ground truth view and compute cross-entropy loss between the projected segmentation map and ground truth.

4.3. Geometric sampling space

Training a *SOF* for every single instance is neither efficient nor useful. Instead, we expect our *SOF* to represent the underlying geometric structure of all portraits while compressing their variety into the low dimensional geometric code z. For this purpose, we build a dataset D with 664 portrait scans and plug a shared hyper-network $\mathcal{H}$ controlled by a m-dimensional latent vector z into *SOF* to generate parameters for each Φ_i:

$$\mathcal{H} : \mathbb{R}^m \to \mathbb{R}^{\|\Phi\|}, \quad z^i \mapsto \Phi_i, i \in [1, ..., M] \qquad (4)$$

where i refers to the ith instance in $\mathcal{D}$. As z is linear-interpolatable, each subset of zs defines a geometry sampling space.

$$\mathcal{G}_{SOF} = \{z_s^j | j \in J, J \subseteq [1, ..., M]\} \qquad (5)$$

Therefore new instances can be obtained by linearly interpolating a set of random selected bases $\mathcal{B}$ from $\mathcal{G}_{SOF}$,
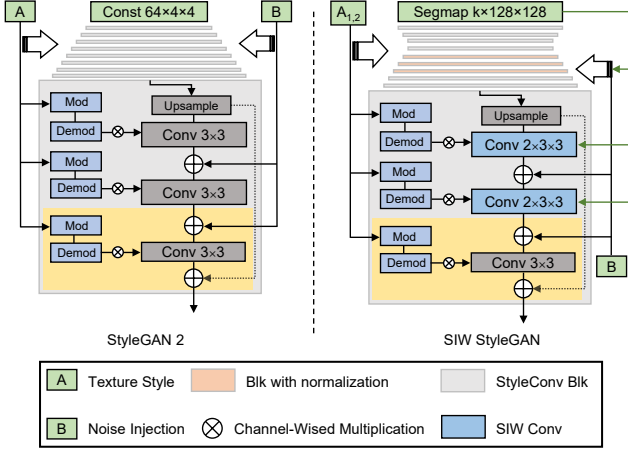
Figure 4. Generator structure. Left: our baseline StyleGAN2 image generator, right: the proposed SIW StyleGAN generator.

$$\Phi_x = \mathcal{H}(z_x) = \sum_{z_i \in \mathcal{B} \subseteq \mathcal{G}_{SOF}} w_i z_i, \quad \text{where} \sum w_i = 1 \tag{6}$$

While w_i could ideally be any real-value, constraining $\sum w_i = 1$ preventing the interpolated code exceeding the given *SOF* space.

5. Texturing with SIW styleGAN

Image stylize from semantic maps is a well-known Image-to-Image translation problem[10, 37, 36, 21, 38]. In the following section, we introduce a new regional unpaired image-to-image translation architecture, enabling us to dynamically adjust both global and local styles from a given semantic map. We call our new architecture SIW StyleGAN. Unlike the original StyleGAN generator that generates images as a whole, SIW StyleGAN stylizes each semantic region separately according to a semantic segmentation map.

5.1. SIW styleGAN Architecture

We formulate the regional styling process for segmentation map $\mathcal{M}$ with style code z as $G(z, \mathcal{M})$. As shown in Fig. 4, the baseline StyleGAN2 starts the synthesis from learned 4×4 constant blocks under various resolutions ($4^2 - 1024^2$), since low resolutions are meaningless for regional styling, we replace the constant blocks with a three-layer encoder to diminish the the *phase* artifacts [13] (i.e. spatial coherence of attributes and its pixel coordinate).

Then, we mix randomly sampled style codes into each semantic region for regional styling. A nature implementation is to extend the original style modulation[13] into K dimension based on the style code z and semantic map $\mathcal{M}$:

$$\mathcal{F}_{o_{uv}} = \mathcal{F}_{in_{uv}} \otimes \sum_k \mathcal{M}(u, v) \cdot w'_{kijl} \tag{7}$$

$$w'_{kijl} = s_{ki} \times w_{ijl}$$

Where w and w' are the original and modulated weights, $\mathcal{M}(u, v)$ is one hot semantic label of the pixel u, v, s_{ki} is the scales of the kth semantic region's ith input feature maps, i, j, l enumerate the input, output feature maps and spatial footprint of the convolution respectively.

As pixel-wised convolution require content switch, the $k-$dimensional modulation is inefficient for training. We instead use a more direct way in *SIW*, i.e. the SIW styleConv. Unlike styleGANs mixing styles on coarse to fine layers, SIW styleConv mix styles spatially with two similarity maps $\mathcal{SM}$, each semantic region shares a same similarity in $\mathcal{SM}$. For each forward pass, we randomly sample two styles $\mathcal{W}_0$ and $\mathcal{W}_1$ (A_0 and A_1 as shown in Fig.4), then assign for each semantic area a random number p as probability to styling from $\mathcal{W}_0$ and $1.0 - p$ from $\mathcal{W}_1$, we output a mixed feature maps $\mathcal{F}_o$ with:

$$\mathcal{F}_o = \gamma \cdot (\mathcal{F}_{in} \otimes \mathcal{W}'_0 \cdot \mathcal{SM} + \mathcal{F}_{in} \otimes \mathcal{W}'_1 \cdot (1.0 - \mathcal{SM})) + \beta \tag{8}$$

where the γ, β are the variance and mean of spatially adaptive normalization(SPADE)[21]. We regenerate the similarity maps $\mathcal{M}$ once for each forward path, and share it to all SIW styleConv Blocks.

As shown in the right side of Fig.4, our generator starts from one hot semantic segmentation maps $k \times 128^2$, passing through 3 SIW StyleConv blocks and downscale to 256×16^2 features maps. Note that we discard the noise inputs in StyleGANs, since noise does not contribute to extraction of semantic features. We only use SPADE [21] in $64^2 - 256^2$ layers and does not apply the "ToRGB" block(yellow area) as we found this would flatten the variety of texture styles.

We train SIW StyleGAN with non-saturating loss [6] with R1 regularization [17] as in the original StyleGANs.

6. Experiments

In the following, we discuss quantitative and qualitative results of our image generation framework.

6.1. Datasets

We use the following datasets in our experiments: 1) CelebAMask-HQ [16] containing 30000 segmentation masks for the CelebAHQ face image dataset. There are 19 different region categories, we merge left/right labels to the same label and subdivide nose into the left and right region into our data prepossessing. 2) FFHQ [12] contains 70000 high-quality images and we label its semantic classes with
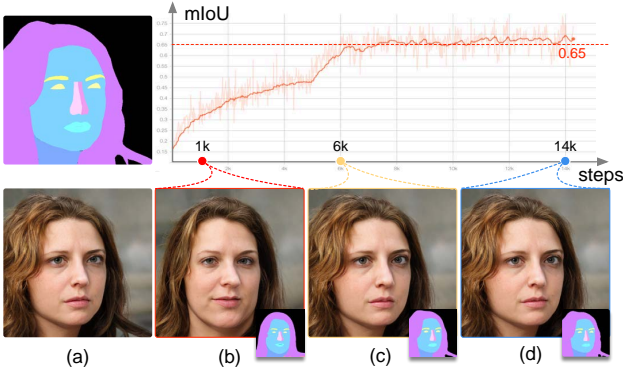
Figure 5. Evaluation of *SOF* on CelebAMask-HQ. (a) Ground truth segmentation (top) and generated image (bottom). (b,c,d) Generated images from optimized segmentation maps with 1k/6k/14k optimization steps.

an existing face parser [2]. 3) 3D portrait mesh, to train our semantic implicit fields, we synthesis multi-view semantic segmentation maps from about 1000 3D scans collecting from AVATAR SDK [3].

6.2. Implementation details.

Training SOF. We follow the structure of SRNs [31] and compose our *SOF* with three submodules. The ray marcher is same with SRNs. The hyper-network $\mathcal{H}$ in Eq. 4 contains one hidden layer with 256 channels, and generate a scene representor Φ for each instance as a 4 layer FC with input channel $m = 256$. The classifier is simply a FC layer with 256 input channels and k output channels, as in Eq. 3.

We train *SOF* on NVIDIA Quadro P6000 with 24G GPU memory. We use an Adam optimizer with linear warm-up and cosine decay. The peak learning rate is $1e - 4$. It takes about 1.5 days to train *SOF* with 3k face instances.

Expand the sampling space. As you may notice, since *SOF* is instance-based, the size of the geometric sampling space is greatly constrained by the size of training dataSet $\mathcal{D}$. While the acquisition of multi-view segmentation map is rather expansive, using in-the-wild segmented images, we must face two major obstacles:

- *SOF* depends on multi-view inputs, while most in-the-wild images have only one view input for each instance.

- As a well-trained *SOF* encodes a unique world coordinate depends on the training set, calibrate in-the-wild image into *SOF* coordinate remains challenging.

Inspired by the one-shot training in SRNs [31], we introduce a two-round training of *SOF*. During the first round,

we train *SOF* Avatar dataSet, which contains 3714 face instances and 20 segmentation maps for each view; During the second round, we fix parameters of all the three modules in *SOF*, and concatenate the geometric code z_j in Eq.5 with a 3D camera pose parameter $c = (x, y, z) \in \mathbb{R}^3$, which represents camera position in the trained *SOF* world coordinate. We jointly optimize c and z on CelebAMask-HD [16] for 200000 steps. We evaluate the quality of the optimized segmentation map in Fig. 5. The Avatar dataSet lacks details compared with manually labelled CelebAMask-HD [16], it's generally hard to optimize high-frequency details from the trained *SOF*. Thus, after 8000 iterations in the second round, when the contour of an optimized segmentation map and the given segmentation map are generally aligned, we re-activate the three modules and optimize the whole network in the following iterations.

Training SIW StyleGAN image generator is similar with official StyleGAN2[13], including the dimensionality of Z and W (512), mapping network architecture(8 fully connected layers), leaky ReLU activation with $\alpha = 0.2$, exponential moving average of generator weights[13], style mixing regularization [12], non saturating logistic loss[6] with R1 regularization [17], Adam optimizer[14] with the same hyper parameters($\beta_1 = 0, \beta_2 = 0.99, \epsilon = 10^{-8}$), and training dataSets.

We performed all training with path regularize every 8 steps, style mixing $p = 0.9$, data augmentation with random scale($1.0 - 1.7$) and crop, we re-implement the official TensorFlow implementation of StyleGAN[4] with Pytorch 1.5.0[22]. our model(at 1024×1024 resolution, total 10000 kimg) is trained with 4 RTX 2080 Ti GPUs and CUDA 10.1, which takes about 22 days.

6.3. Ablation Study on SIW StyleGAN

To better analyze the role of each part of our SIW Style-GAN, we conduct an ablation study on 1) Constant input vs. semantic maps encoder and 2) with vs. without SIW mix style training. The ablation study checkpoints are trained with $800K$ steps under 1024^2 resolution.

Constant input vs. encoder Unlike StlyGAN2 target on synthesis static images as real as possible, our generator attempts to enable some new effects including dynamic local and global styling, free viewport generation. We observe constant input would cause two obvious artifacts: 1) The phase artifacts, as shown in Fig.8, i.e., strong localize appearance, which is especially noticeable when we change our perspective(demonstrate in our video), We pinpoint the problem to the constant input strengthen the constant spatial effect. 2) The styles "scuffle" artifacts, i.e., our output depend on both styles and semantic map and the styles, constant input architecture result in the styles, and semantic contour are totally independent to each other, we ob-
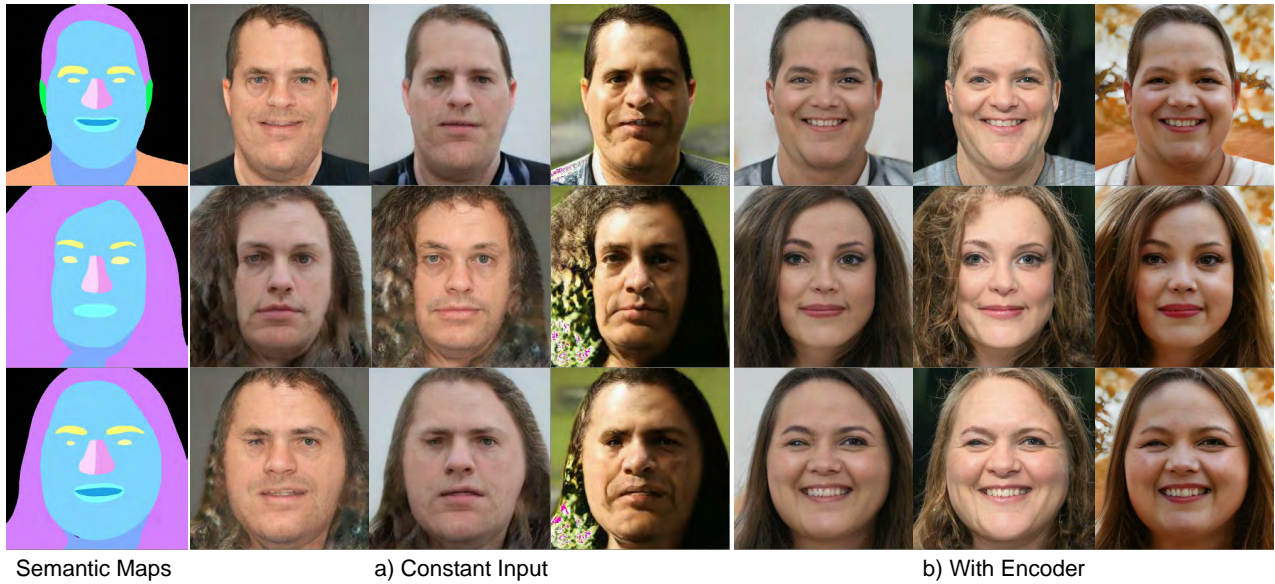

Figure 6. With vs. without encoder, each column uses a same style. a) $512 \times 4 \times 4$ constant input, b) $17 \times 128 \times 128$ one hot semantic maps downscale to $128 \times 16 \times 16$ with SIW StyleConv block
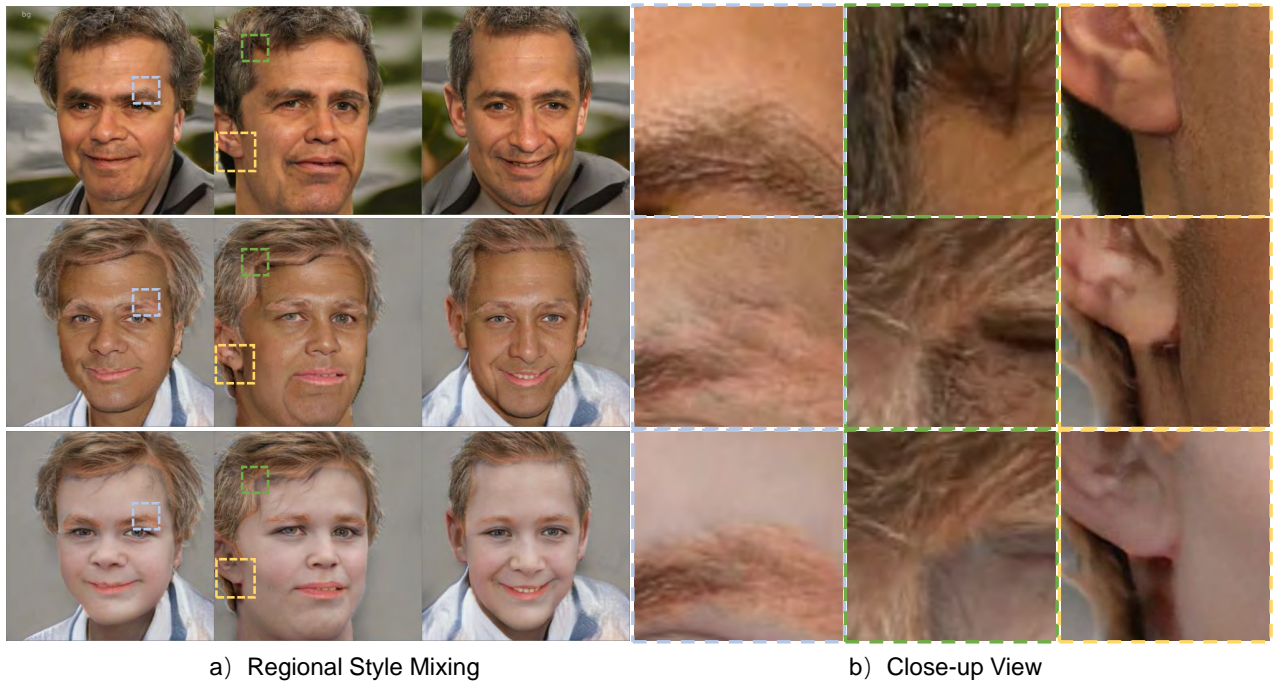

Figure 7. With vs. without mix style training, each row uses a same style. First row: mix style results with SIW mix style blocks, 2-4th row: mix styles results without SIW mix style blocks.

serve that they are usually incomparable to each other, i.e., feeding a woman's semantic map and man's texture styles would lead to significant artifacts(shown (a) of Fig.6), however, our dynamic changing input strategy enhance the connection between styles and semantic map, can efficient re-

duce this incompatibility, as shown (b) of the Fig.6, but still haven't resolved it, as discussed in the limitation section.

With vs without SIW mix style training. To enable regional stylize effect, we purpose a spatial mix style training strategy, a comparison baseline is to training the generator

	INPUTS		TRAINING	EFFECTS		
	latent code	segmentation	pairwised	global style	local style	free view
Pix2PixHD[36]	√	√	√			
SPADE[21]	√	√	√	√		
SEAN[38]	√	√	√	√	√	
StyleGAN2[13]	√			√		
SIW StyleGAN	√	√		√	√	√

Table 1. Comparison of required inputs and enabled effects.

Figure 8. The "phase" artifact.

Figure 9. Quantitative evaluation on CelebA[16] and FFHQ[12] dataSet.

with the layered mix style and spatially mix multiply styles with the semantic maps, as $2 − 4$ rows of the Fig.7, we can observe significant artifacts on the semantic boundary and overall image looks unnatural. While with mix style training can create soft the semantic boundary and produce a reasonable result even given different styles. We refer the readers to the supplementary material for more results.

6.4. Quantitative evaluation.

We compare Frchet Inception Distance(FID)[8] with most recent image synthesis methods: Pix2PixHD[36], SPADE[21], SEAN[38] and the baseline StyleGAN2[13] for quantitative evaluation. Table 1 compares the requirements and enabled visual effects of our SIW StyleGAN and the baseline methods. Our SIW StyleGAN is the only one which enables both global and local style synthesis effects while do not require paired data (segmentation map and rgb image) for training.

To be fair, we retrain all the models on FFHQ[12] and CelebA[11] dataset with $800k$ iterations under 512^2 resolution, we use another dataset as evaluation set when training with one of the above dataset, and we set $truncation = 1.0$ when evaluation. We calculate FID value of $50k$ images once per $100k$ steps. Result is shown in Fig. 9, we achieve the state-of-the-art with lower FID value[5].

Compared with SPADE and SEAN, our styles codes are

sampled directly from high dimensional random noise instead of encoded from conditional images, bring more freedom to the style space, thus increase the variety in generated images. Moreover, our training speed is much faster than the styleGAN2 baseline, one possible reason could be the semantic segmentation map disentangles the whole texture space into regions with similar color distribution, leading the generator to converge faster. Appendix D gives a visual comparison.

Fig.14 and Fig.15 show visual comparison of our method with SOTA image synthesis methods: Pix2PixHD[36], SPADE[21], SEAN[38] and StyleGAN2[13] trained on CelebAMask-HQ [16] and FFHQ [12]. We train each network for $800k$ steps, and the sampled images are all under 512×512 resolution. Since some baseline methods require pair-wise input, we firstly project images in the training dataset onto texture space to acquire style code for each image, then we randomly pick images that has the same semantic classes with the reference segmentation from the training dataset, and use their style code for generation. From the visual comparison, we can see that images generated by our framework are richer in texture than those generated by Pix2PiXHD and SPADE, more realistic compared with SEAN results; and are locally-editable while achieving comparable quality with StyleGAN2 generated images.

6.5. Applications

As mentioned before, the generation process is controlled by three variables, camera pose $C[R, T, K]$, a geometric code z and a style code z', changing each of them separately leads enables a series of effects.

---

[5]The result for baseline methods might be slightly different from their original papers, as we use random styles for evaluation.
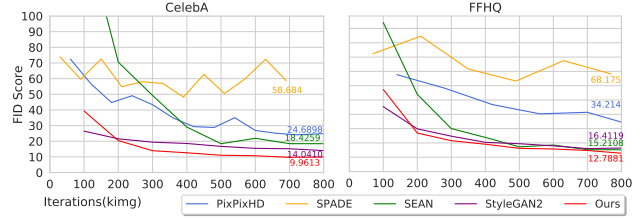
Figure 10. Results. Top: semantic-level styles adjustment, bottom: semantic maps generated from SOF with camera controlling and image synthesis with different styles.

Free-Viewpoint Synthesis. As demonstrated in Fig. 10 (bottom), given a set of camera poses and a geometric code z, we can firstly query a set of 2D segmentation maps according to the given camera poses (last row). We are then texturing on the 2D segmentation maps with a style code z' to generate photo-realistic images.

Global and Local Style Adjustment. By adjusting the style similarity map $\mathcal{SM}$ we can achieve both global and lo-

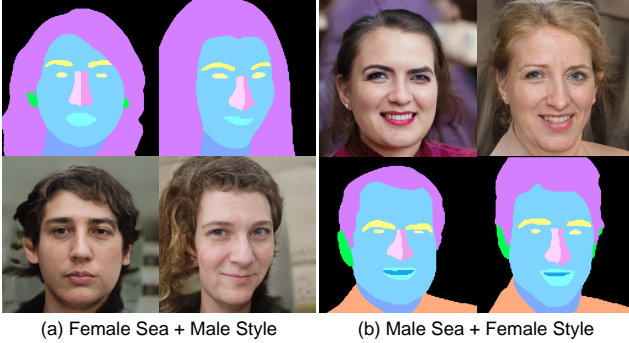(a) Female Sea + Male Style   (b) Male Sea + Female Style

Figure 11. Reprojection error cased by gender ambiguity.

cal style control. As shown in Fig. 10 (top), we could adjust styles in each semantic region separately, while maintaining the global style and illumination. From the close-ups, we can also conclude that our SIW StyleGAN can fix seams and unnatural lighting caused by local style change.

To better demonstrate the performance of our method, we further iterated 10000 kimg at 1024^2 resolution on FFHQ dataset and evaluate with CelebAMask-HQ semantic maps. Fig.12 shows additional global styles adjustment results, Fig.13 shows regional style adjustment.

7. Limitations and Discussions

In this paper, we presented a novel two stages portrait image synthesis framework that enables 3D and semantic-level controllable, to be specific, we propose an implicit semantic field and semantic instance wised StyleGAN to model geometric and texture achieve appearance consistency shape, poses controlling, global and local styles adjustment. We also presented an unsupervised training scheme in the SIW StyleGAN module that relax the pairwise constrain between semantic map and target outputs and reach SOTA performance of FID Score evaluation in CelebA and FFHQ dataSet.

Since the geometry and texture are sampled independently, conflicts might occur if there is a gender mismatch between the semantic contour and styles. For example, in Fig.11, when applying a male style to female segmentation map, the generator may paint background texture onto hair region to match the texture distribution of male; conversely, when applying female style onto male segmentation, the generator would paint hair-like texture onto the background. Such artifacts may originate from the discriminator since it's not regional aware and only expects the global texture distribution of the generated image is similar to training data. One possible solution is to re-design the discriminator to enhance regional discrimination.

References

[1] Volker Blanz and Thomas Vetter. A morphable model for the synthesis of 3d faces. In *Proceedings of the 26th annual conference on Computer graphics and interactive techniques*, pages 187–194. ACM Press/Addison-Wesley Publishing Co., 1999. 2

[2] Xi Chen, Yan Duan, Rein Houthooft, John Schulman, Ilya Sutskever, and Pieter Abbeel. Infogan: Interpretable representation learning by information maximizing generative adversarial nets. In *Advances in neural information processing systems*, pages 2172–2180, 2016. 1

[3] Zhiqin Chen and Hao Zhang. Learning implicit fields for generative shape modeling. In *Proceedings of the IEEE Conference on Computer Vision and Pattern Recognition*, pages 5939–5948, 2019. 1, 2, 4

[4] Edo Collins, Raja Bala, Bob Price, and Sabine Süsstrunk. Editing in style: Uncovering the local semantics of GANs. In *IEEE Conference on Computer Vision and Pattern Recognition (CVPR)*, 2020. 2

[5] Yu Deng, Jiaolong Yang, Dong Chen, Fang Wen, and Xin Tong. Disentangled and controllable face image generation via 3d imitative-contrastive learning. *ArXiv*, abs/2004.11660, 2020. 1

[6] Ian Goodfellow, Jean Pouget-Abadie, Mehdi Mirza, Bing Xu, David Warde-Farley, Sherjil Ozair, Aaron Courville, and Yoshua Bengio. Generative adversarial nets. In *Advances in neural information processing systems*, pages 2672–2680, 2014. 1, 2, 5, 6

[7] David Ha, Andrew M. Dai, and Quoc V. Le. Hypernetworks. *ArXiv*, abs/1609.09106, 2017. 4

[8] Martin Heusel, Hubert Ramsauer, Thomas Unterthiner, Bernhard Nessler, and Sepp Hochreiter. Gans trained by a two time-scale update rule converge to a local nash equilibrium. In *Advances in neural information processing systems*, pages 6626–6637, 2017. 8

[9] Phillip Isola, Jun-Yan Zhu, Tinghui Zhou, and Alexei A Efros. Image-to-image translation with conditional adversarial networks. In *Proceedings of the IEEE conference on computer vision and pattern recognition*, pages 1125–1134, 2017. 2

[10] Phillip Isola, Jun-Yan Zhu, Tinghui Zhou, and Alexei A Efros. Image-to-image translation with conditional adversarial networks. In *Proceedings of the IEEE conference on computer vision and pattern recognition*, pages 1125–1134, 2017. 2, 5

[11] Tero Karras, Timo Aila, Samuli Laine, and Jaakko Lehtinen. Progressive growing of gans for improved quality, stability, and variation. *arXiv preprint arXiv:1710.10196*, 2017. 2, 8

[12] Tero Karras, Samuli Laine, and Timo Aila. A style-based generator architecture for generative adversarial networks. In *Proceedings of the IEEE Conference on Computer Vision and Pattern Recognition*, pages 4401–4410, 2019. 1, 2, 5, 6, 8, 17

[13] Tero Karras, Samuli Laine, Miika Aittala, Janne Hellsten, Jaakko Lehtinen, and Timo Aila. Analyzing and improving the image quality of stylegan. *arXiv preprint arXiv:1912.04958*, 2019. 1, 2, 5, 6, 8

[14] Diederik P Kingma and Jimmy Ba. Adam: A method for stochastic optimization. *arXiv preprint arXiv:1412.6980*, 2014. 6

[15] Line Kuhnel, Tom Fletcher, Sarang Joshi, and Stefan Sommer. Latent space non-linear statistics. *arXiv preprint arXiv:1805.07632*, 2018. 2

[16] Cheng-Han Lee, Ziwei Liu, Lingyun Wu, and Ping Luo. Maskgan: Towards diverse and interactive facial image manipulation. In *IEEE Conference on Computer Vision and Pattern Recognition (CVPR)*, 2020. 1, 2, 5, 6, 8, 16

[17] Lars Mescheder, Andreas Geiger, and Sebastian Nowozin. Which training methods for gans do actually converge? *arXiv preprint arXiv:1801.04406*, 2018. 5, 6

[18] Lars Mescheder, Michael Oechsle, Michael Niemeyer, Sebastian Nowozin, and Andreas Geiger. Occupancy networks: Learning 3d reconstruction in function space. In *Proceedings of the IEEE Conference on Computer Vision and Pattern Recognition*, pages 4460–4470, 2019. 1, 2

[19] Michael Oechsle, Michael Niemeyer, Lars M. Mescheder, Thilo Strauss, and Andreas Geiger. Learning implicit surface light fields. *ArXiv*, abs/2003.12406, 2020. 3

[20] Jeong Joon Park, Peter Florence, Julian Straub, Richard Newcombe, and Steven Lovegrove. Deepsdf: Learning continuous signed distance functions for shape representation. In *Proceedings of the IEEE Conference on Computer Vision and Pattern Recognition*, pages 165–174, 2019. 1, 2, 3, 4

[21] Taesung Park, Ming-Yu Liu, Ting-Chun Wang, and Jun-Yan Zhu. Semantic image synthesis with spatially-adaptive normalization. In *Proceedings of the IEEE Conference on Computer Vision and Pattern Recognition*, 2019. 2, 5, 8

[22] Adam Paszke, Sam Gross, Francisco Massa, Adam Lerer, James Bradbury, Gregory Chanan, Trevor Killeen, Zeming Lin, Natalia Gimelshein, Luca Antiga, et al. Pytorch: An imperative style, high-performance deep learning library. In *Advances in neural information processing systems*, pages 8026–8037, 2019. 6

[23] Songyou Peng, Michael Niemeyer, Lars M. Mescheder, Marc Pollefeys, and Andreas Geiger. Convolutional occupancy networks. *ArXiv*, abs/2003.04618, 2020. 3

[24] Stanislav Pidhorskyi, Donald A Adjeroh, and Gianfranco Doretto. Adversarial latent autoencoders. In *Proceedings of the IEEE Computer Society Conference on Computer Vision and Pattern Recognition (CVPR)*, 2020. [to appear]. 2

[25] Olaf Ronneberger, Philipp Fischer, and Thomas Brox. U-net: Convolutional networks for biomedical image segmentation. In *International Conference on Medical image computing and computer-assisted intervention*, pages 234–241. Springer, 2015. 2

[26] Shunsuke Saito, Zeng Huang, Ryota Natsume, Shigeo Morishima, Angjoo Kanazawa, and Hao Li. Pifu: Pixel-aligned implicit function for high-resolution clothed human digitization. *2019 IEEE/CVF International Conference on Computer Vision (ICCV)*, pages 2304–2314, 2019. 3

[27] Hang Shao, Abhishek Kumar, and P Thomas Fletcher. The riemannian geometry of deep generative models. In *Proceedings of the IEEE Conference on Computer Vision and Pattern Recognition Workshops*, pages 315–323, 2018. 2

[28] Yujun Shen, Jinjin Gu, Xiaoou Tang, and Bolei Zhou. Interpreting the latent space of gans for semantic face editing. *arXiv preprint arXiv:1907.10786*, 2019. 2

[29] Yujun Shen, Ceyuan Yang, Xiaoou Tang, and Bolei Zhou. Interfacegan: Interpreting the disentangled face representation learned by gans. *arXiv preprint arXiv:2005.09635*, 2020. 1

[30] Karen Simonyan and Andrew Zisserman. Very deep convolutional networks for large-scale image recognition. *arXiv preprint arXiv:1409.1556*, 2014. 2

[31] Vincent Sitzmann, Michael Zollhöfer, and Gordon Wetzstein. Scene representation networks: Continuous 3d-structure-aware neural scene representations. In *NeurIPS*, 2019. 1, 3, 4, 6

[32] Tiancheng Sun, Jonathan T Barron, Yun-Ta Tsai, Zexiang Xu, Xueming Yu, Graham Fyffe, Christoph Rhemann, Jay Busch, Paul Debevec, and Ravi Ramamoorthi. Single image portrait relighting. *ACM Transactions on Graphics (Proceedings SIGGRAPH)*, 2019. 2

[33] Ayush Tewari, Mohamed Elgharib, Gaurav Bharaj, Florian Bernard, Hans-Peter Seidel, Patrick Pérez, Michael Zollhöfer, and Christian Theobalt. Stylerig: Rigging stylegan for 3d control over portrait images. *arXiv preprint arXiv:2004.00121*, 2020. 1, 2

[34] Paul Upchurch, Jacob Gardner, Geoff Pleiss, Robert Pless, Noah Snavely, Kavita Bala, and Kilian Weinberger. Deep feature interpolation for image content changes. In *Proceedings of the IEEE conference on computer vision and pattern recognition*, pages 7064–7073, 2017. 2

[35] Ting-Chun Wang, Ming-Yu Liu, Jun-Yan Zhu, Andrew Tao, Jan Kautz, and Bryan Catanzaro. High-resolution image synthesis and semantic manipulation with conditional gans. In *Proceedings of the IEEE conference on computer vision and pattern recognition*, pages 8798–8807, 2018. 2

[36] Ting-Chun Wang, Ming-Yu Liu, Jun-Yan Zhu, Andrew Tao, Jan Kautz, and Bryan Catanzaro. High-resolution image synthesis and semantic manipulation with conditional gans. In *Proceedings of the IEEE Conference on Computer Vision and Pattern Recognition*, 2018. 2, 5, 8

[37] Jun-Yan Zhu, Taesung Park, Phillip Isola, and Alexei A Efros. Unpaired image-to-image translation using cycle-consistent adversarial networks. In *Proceedings of the IEEE international conference on computer vision*, pages 2223–2232, 2017. 5

[38] Peihao Zhu, Rameen Abdal, Yipeng Qin, and Peter Wonka. Sean: Image synthesis with semantic region-adaptive normalization. In *Proceedings of the IEEE/CVF Conference on Computer Vision and Pattern Recognition*, pages 5104–5113, 2020. 1, 2, 5, 8

Figure 12. Global styles adjustment.

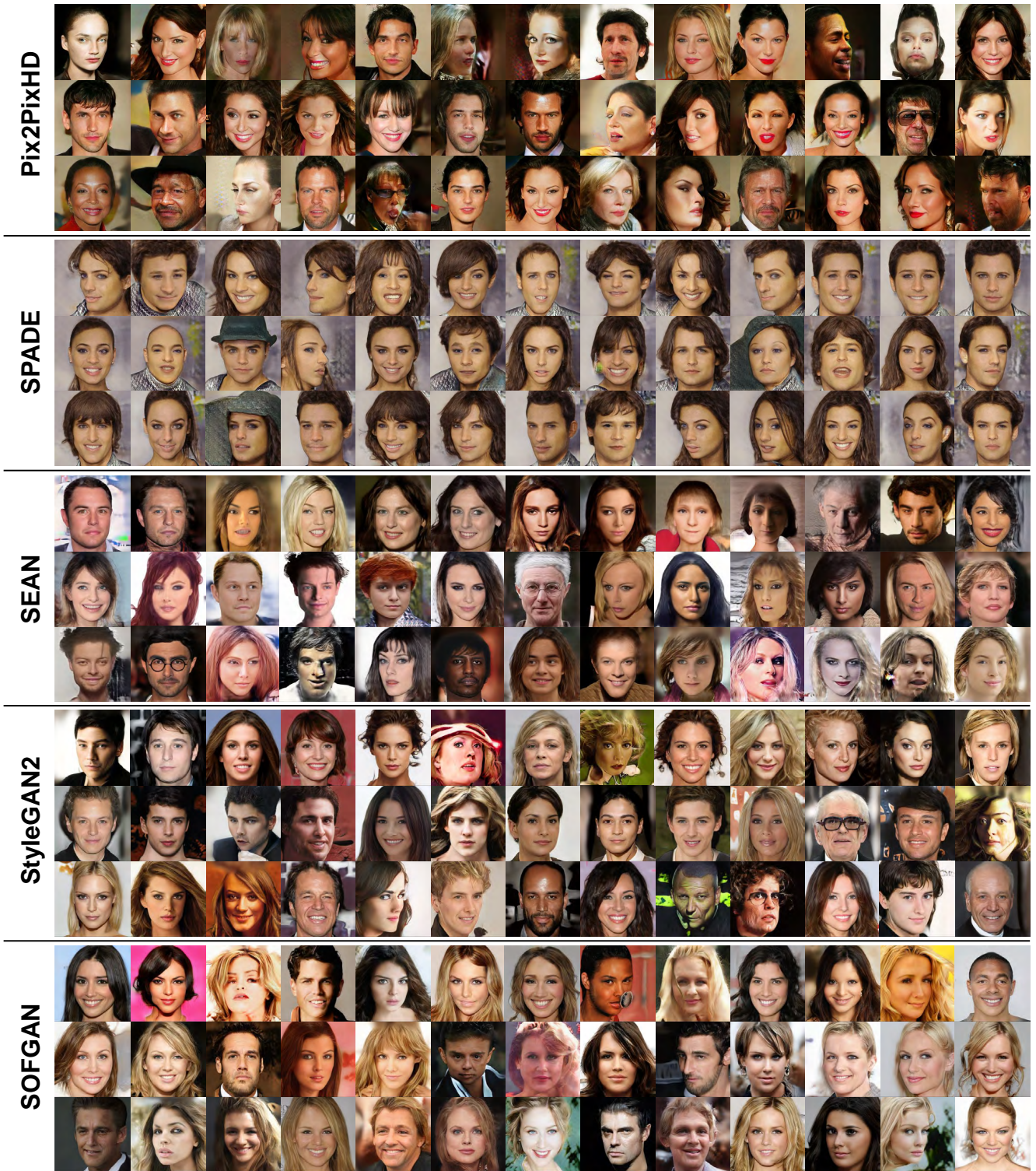Figure 13. Regional styles adjustment.

Figure 14. Visual comparison on CelebAMask-HQ dataset[16], trained with $800k$ images in resolution 512^2.

Figure 15. Visual comparison on FFHQ dataset[12], trained with $800k$ images in resolution 512^2.